Effects of fuel composition at varying air-fuel ratio on knock resistance during spark-ignition combustion

Ahmad Almaleki[1,2], Paul Hellier[2], Nicos Ladommatos[2], Midhat Talibi[2] and Zuhaib Khan[2]

[1]Energy and Water Research Institute, King Abdulaziz City for Science and Technology (KACST), P.O. Box 6086, Riyadh 11442, Saudi Arabia.

[2]Department of Mechanical Engineering, University College London, Torrington Place, London, WC1E 7JE, UK.

*Corresponding author: Ahmad Almaleki, aalmaleki@kacst.edu.sa

Keywords: air-fuel ratio, knock resistance, spark-ignition engines, primary refence fuel, gasoline fuel, RON, variable compression engine, paraffinic fuels, aromatic fuels.

Abstract

Knock resistance of liquid fuels for spark-ignition engines is determined using standardised tests (RON and MON), however, these do not involve consistent control of the air-fuel ratio (λ). In contrast, modern engines have a highly controlled air-fuel λ ratio, often operating in a very narrow range around stoichiometric in order to reduce pollutant emissions and achieve high thermal efficiencies. Hence, understanding the effect of λ on knock resistance of the fuel is imperative.

This paper investigates the influence of varying equivalence air-fuel ratio λ on the knock resistance of a range of fuels of equal RON values but differing chemical

composition. Binary component primary reference fuels and practical gasolines were tested with a Ricardo E6 variable compression engine operated at conditions similar to those used for RON tests. It was found that the knock resistance depended on the air-fuel ratio at which the engine was operated and the chemical composition of the test fuel. For all fuels, the knock resistance became insensitive to compression ratio at stoichiometric and very rich mixtures (λ=1 and λ<0.88). However, the knock resistance of highly paraffinic fuels was observed to be more sensitive to changes in λ than highly aromatic fuels.

1 Introduction

In spark-ignition engines, knock is an abnormal combustion event in which significant thermal energy can be undesirably released, potentially leading to severe engine mechanical damage or reducing engine operating life, performance, and efficiency (Hamilton and Cowart, 2008, Wang *et al.*, 2017). Knock is a major obstacle in the further improvement of SI engines. For example, the onset of knock limits the possibility of increasing the operating compression ratio, or applying turbocharging and downsizing strategies, that enhance thermal efficiency and power density of SI engines. Such strategies lead to an increase in pressure and temperature in the unburned mixture ahead of the flame front, accelerating the auto-ignition in the end-gas and causing knock (Ratcliff *et al.*, 2018).

In spark-ignition engines, knock occurs during flame propagation when the temperature of the unburned gases rises rapidly, exceeding the self-ignition temperature. Many mechanisms can therefore contribute to initiating knock. The overall temperature of the in-cylinder contents changes in response to the piston movement as it compresses or expands the volume of the cylinder contents. The expansion of post-combustion gases compresses the unburned gases, elevating their temperatures. The unburned gas also receives radiation from the burned gas and the surrounding combustion chamber walls. If the local temperature of the unburned gases in the end-gas exceeds the mixture self-ignition temperature, knocking combustion due to end-gas auto-ignition occurs. Thus, gas pressure oscillations and an audible ringing sound caused by reflecting pressure waves driven by the sudden release of energy are observed (Syrimis and Assanis, 2003, Coetzer *et al.*, 2006, Zhen *et al.*, 2012).

Liquid fuels for spark-ignition engines are selected partly based on their ability to resist knock, which is usually expressed through their octane number (ON). The term ON was introduced in 1928 as a standardised measurement and specification of a fuel's resistance to auto-ignition (Stradling *et al.*, 2016; AlAbbad *et al.*, 2017; Kalghatgi and Stone, 2018). Fuels with a higher octane number can be more resistant to auto-ignition and thus are often used in higher compression ratio engines. The octane number concept has since been adopted globally for quantitative knock determination of liquid fuels for spark-ignition engines, utilising standardised equipment, a cooperative fuel research (CFR) engine, and the two following different sets of standardised operating conditions. The first set of operating conditions is used to evaluate the knock rating of fuels under mild operating conditions and provide a fuel parameter called the Research Octane Number (RON), while the second set is performed to rate a fuel under severe operating conditions and obtain the Motor Octane Number (MON). Table 1 shows the operating conditions of RON and MON tests. Overall, fuels are rated for MON at a higher intake mixture temperature and a higher engine operating speed than RON tests, representing more severe engine operating conditions (Kolodziej and Wallner, 2017). Therefore, during MON rating, the temperature of unburned gas is considerably higher at a given pressure than that under RON conditions. Hence, practical fuels always have lower MON values than RON, typically 10 values lower (Stradling *et al.*, 2016). The difference between these two measured parameters (RON – MON) is known as fuel sensitivity (S) (Kalghatgi and Stone, 2018).

Table 1: RON and MON engine operating conditions.

Parameter	**RON**	**MON**
Intake air temperature	52 ºC	149 ºC
Intake air pressure	Atmospheric	
Coolant temperature	100 ºC	
Engine speed	600 rpm	900 rpm
Spark timing	13 °BTDC	14-26 °BTDC
Compression ratio	4 to 18	

In spark-ignition engines, the variation of equivalence air-fuel ratio (λ) has a direct influence on the occurrence and intensity of knock (Brock and Stanley, 2012). For a test or sample fuel, RON and MON are determined in a CFR engine at a relative air-fuel ratio of the mixture that produces the highest knock intensity. By using the falling level technique, the carburettor fuel level can be changed from a high or rich mixture condition to a low or lean mixture condition to reach the standardised knock intensity

(ASTM Int., 2019). However, this relative air-fuel ratio value cannot be quantified, and it is not known if the knock characteristics of test and sample fuels are compared at similar operating λ. In contrast, modern engines have a highly controlled λ ratio, often operating in a very narrow range around stoichiometric to reduce pollutant emissions and achieve high thermal efficiencies. Hence, understanding the effect of the equivalence air-fuel ratio λ on the knock resistance of a fuel is imperative, especially for future fuels that will potentially be derived from non-conventional sources, possessing a different chemical composition and a reduced variety of components.

The effects of the variation of equivalence air-fuel ratio λ and chemical composition of spark-ignition fuels have been investigated in several studies. Huber *et al.*, (2013) examined the standardised octane rating methods for RON and MON determination to develop a new engine-based test method that could better fit with modern engine technologies. It was observed that the variation of λ highly affected the ignition and combustion characteristics of the test fuels. Paraffinic primary reference fuels displayed different ignition and combustion characteristics than conventional gasoline. The variation of λ was also shown to have a significant impact on the resultant knock intensity of these test fuels. However, the effect was not explicitly investigated, and insufficient understanding about the behaviour of these fuels on a commercial gasoline engine operating at a fixed air-fuel ratio was obtained.

(Kolodziej and Wallner, 2017) investigated the effects of varying λ on the knocking characteristics and RON rating of a range of fuels all with a RON of 98 but with varying composition (achieved through different proportions of iso-paraffinic and aromatic species and also ethanol). It was found that the knock tendency of PRFs reduced significantly as the mixture moved towards stoichiometric, displaying greater knock resistance in comparison to aromatic and ethanol blends of the same RON values. The results indicated that PRFs are more sensitive to changes in λ ratios than conventional gasoline fuels. A similar significant sensitivity in the combustion characteristics of PRF corresponding to a change in the rate of fuel supply was also reported by (Dec and Sjöberg, 2004) studying the effect of fuel chemistry on combustion phasing and ignition control of a single cylinder direct injection HCCI engine. In this study, three fuels; pure isooctane, gasoline and PRF 80, were examined. Slight changes in the autoignition characteristics of both isooctane and gasoline during the increase of fuel flow rate were observed compared to the PRF, attributable to the rise in the PRF cool-flame activity while increasing fuel mass flow rate.

(Montoya *et al.*, 2018) studied the effect of varying equivalence air-fuel ratio on knock tendency in two different engine configurations; a CFR unit and a converted Lister Petter TR2 Diesel engine (TR2) that operated as a spark-ignition engine, from lean to stoichiometric. Several fuel blends made of biogas, natural gas, propane, and hydrogen were tested. It was found that in the CFR engine, a lean mixture decreased the knocking tendency. Therefore, the engine could be operated at a higher critical engine compression ratio than a stoichiometric mixture. However, the opposite effect of varying equivalence air-fuel ratios was observed in the converted diesel engine, increasing the knock tendency with the supply of leaner mixtures. This was attributed to the increase in the mixture pressure at the end of engine compression stroke due to increased intake charge density while introducing more air, thus leaner mixture, to the engine. At a fixed and super lean equivalence air-fuel ratio, (Naruke *et al.*, 2020) investigated the effect of fuels with different ignition characteristics on the knock propensity of a single cylinder spark-ignition engine operated at a fixed engine compression ratio of 15:1 and λ of 1.8. It was found that, at the occurrence of knock limit, the octane number and octane index of the fuels investigated did not correlate well with the crank angle position CA50.

While the variation of both equivalence air-fuel ratio λ and fuel composition has been observed to affect knock resistance significantly, there remains a limited systematic understanding of the combined influence of these parameters. Such insights are increasingly necessary with the uptake of alternative fuels and precise control of air-fuel stoichiometry. Therefore, this study investigates the effect of varying air-fuel ratio and fuel composition on knock resistance and knocking combustion characteristics, utilising practical gasoline fuels and PRFs of similar octane rating. All tests were conducted using a single cylinder E6 variable compression ratio spark-ignition engine, operated at standardised conditions similar to those used in RON measurements with consistent control of the air-fuel ratio (λ) and knock limit.

2 Experimental Setup

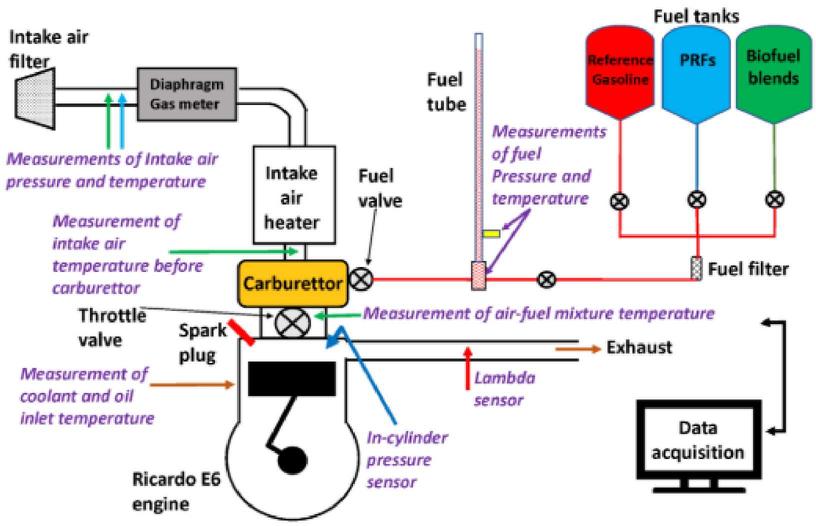

Figure 1: Schematic diagram of the engine test rig and measurement systems.

Figure 1 shows a general layout of the experimental systems utilised in this study. A Ricardo E6 single cylinder variable compression engine (serial number of 98/67) configured for spark ignition combustion, was used for all experiments. The compression ratio of the test engine was manually varied between 4.5:1 and 9.1:1 while the engine was running by increasing or decreasing the relative position of the engine head to the crankshaft. The test engine was coupled to an electric dynamometer of swinging field direct current type. Table 2 summarises the test engine geometry specifications and valves timings.

The air-fuel mixture was prepared via the test engine carburettor (Solex 35 F.A.1) and ignited by a 14 mm spark plug with 0.7mm gap (NGK BPR6HS), situated at the side of the combustion chamber between the valves. To determine the air-fuel ratio λ, an O_2/lambda sensor (ECM AFRecorder 1200), fitted in an M18 hole approximately 120 mm downstream of the engine exhaust valve, was utilised. The O_2/lambda sensor was calibrated for every test using the Hydrogen-to-Carbon (H/C) and Oxygen-to-Carbon (O/C) mass ratios of the test fuel. As the engine was operated at wide-open throttle for all tests, the ratio of the air-fuel mixture was varied and controlled during experiments using the test engine carburettor needle valve.

Several measuring transducers and sensors were installed for acquisition of pressure and temperature readings during tests as follows. Measurements of in-cylinder pressure were taken by a water-cooled piezo-electric pressure transducer (Kistler 6041B) in conjunction with a Kistler 5007 charge amplifier. The in-cylinder pressure measurements were referenced to the intake manifold pressure at a time at which the piston was at BDC and the inlet valve open. Temperature measurements for air, coolant water and lubricant oil were made by K-type thermocouples connected to thermocouple amplifiers of type Adafruit MAX31855 and placed at different positions. For monitoring and controlling the temperature of the air-fuel mixture just before delivery to the engine, a K-type thermocouple was also fitted after the carburettor and connected to a PID box so that the mixture intake temperature could be controlled. The relative humidity of the ambient air was measured using a capacitive humidity sensor type HPP805A031. All signals from the measuring instruments were acquired as analogue inputs by two separate PCs equipped by National Instruments multifunction I/O data acquisition cards with a high-speed sampling rate of 1.25 MS/s.

Table 2: Geometry specifications of the Ricardo E6 engine.

Number of cylinders	Single cylinder

Compression ratio	Variable from 4.5:1 to 20:1
Cylinder Bore	76.2 mm
Cylinder Stroke	111.13 mm
Swept Volume	506.8 cm^3
Number of Valves	1 inlet, 1 exhaust
Inlet Valve timing	IVO: 9 CAD BTDC IVC: 35 CAD ABDC
Exhaust Valve timing	EVO: 42 CAD BBDC EVC: 8 CAD ATDC
Cooling system	Water-cooled
Aspiration system	Natural

3 Experimental Methodology

3.1 Knock detection technique

Knocking combustion cycles were detected directly using measurements of in-cylinder pressure. In order to distinguish between knocking and non-knocking cycles, the in-cylinder pressure signal was filtered by a bandpass filter according to the filter settings summarised in Table 3. The knock index MAPO, as described in Equation 1, was then obtained and compared to a pre-determined threshold of 0.5 bar, a value used in a previous study by (Kalghatgi, 2018). Therefore, the examined cycle was considered to be a knocking combustion cycle if it displayed an amplitude higher than the predetermined threshold within the filter window (10 CAD BTDC to 90 CAD ATDC). The analysis was applied for 50 consecutive combustion cycles. The percentage ratio between knocking combustion cycles and the total number of measured combustion cycles was calculated to find a term referred to as the knock frequency factor (KFRQ), see Equation 2. Hence, this factor was used as an index parameter in order to find the critical compression ratio of each test fuel at various air-fuel ratios.

$$\text{MAPO (bar)} = \max\,[|incylinder\ pressure|]_{10\ CAD\ BTDC}^{90\ CAD\ ATDC} \qquad \text{Equation 1}$$

$$\text{KFRQ (\%)} = \frac{\text{number of Knocking cycles}}{\text{total number of measured cycles}}\ x\ 100 \qquad \text{Equation 2}$$

Table 3: A summary of the bandpass filter settings for knock detection.

Filter type	Band-pass
Detection window	10 CAD BTDC to 90 CAD ATDC
Low Cut off frequency (Hz)	3600
High Cut off frequency (Hz)	18000
Sampling frequency (Hz)	36000
Threshold for knocking cycle detection (bar)	0.5

3.2 Test procedure

Table 4 summaries the test operating conditions utilised in this work. In general, all experimental work was conducted at conditions similar to the International Standard Test Method for Research Octane Number (RON) of Spark-Ignition Engine Fuel (ASTM Int., 2019), excluding the coolant temperature; this was maintained at 70 ºC during motoring tests following the recommendation of the engine manufacturer as the most suitable condition for engine operation.

Table 4: Test operating conditions.

Operating condition	Value
Inlet pressure	Atmospheric
Inlet air temperature	Based on the atmospheric pressure of the test day
Coolant in temperature	70 ºC ± 1.5
Oil Temperature	55 ºC ± 2
Engine speed and Load	600 rpm and Wide open throttle
Spark timing	13 CAD BTDC
Fuel/Air ratio	Varied between 1.00 and 0.82
Compression ratio	Variable

As shown in Table 4, the engine was always operated at wide open throttle, and fixed engine speed and spark timing of 600 rpm and 13 CAD BTDC, respectively. Each combustion test always started at engine CR of 6.91 and λ of 1. The engine CR was then increased gradually in order to find the CR, at λ=1, that resulted in engine knocking of 10% KFRQ. Next, exhaust lambda λ sweeps in the range from 0.98 to 0.84 with increments of 0.025 were undertaken and the maximum engine CR at each λ point for a higher KFRQ of 30% was determined. The different values of KFRQs selected for t λ=1 and richer mixtures, 10% and 30% respectively, were chosen as it was anticipated that a higher engine CR would be required to instigate knock at stoichiometric conditions and could result in knock events of significantly greater magnitude.

In order to investigate the experimental repeatability during combustion, the engine was fuelled by a reference gasoline fuel (Gasoline 91.3 RON) and operated in combustion mode. 13 repeated tests of this fuel, in combustion mode, were performed on different days throughout the experimental work period at the same set of operating conditions, Table 4, but at a constant engine CR of 6.91. Table 5 shows the variability of readings from the sensors and transduces in addition to the calculated standard deviation for each measurement.

Table 5: Variations of measurement readings and the calculated standard deviation for 13 repeated tests of the reference test fuel Gasoline 91.3.

	Measurement	Min	Max	Mean	±SD
Temperatures [°C]	Coolant in	69.6	76.0	72.7	2.0
	Oil	52.5	57.3	54.8	1.3
	Air before carburettor*	47.0	48.5	47.8	0.8

	Exhaust gas	445.3	506.4	477.3	21.4
	Fuel	16.9	19.9	18.8	0.8
	Room	18.8	22.7	20.7	1.0
Relative Humidity	Relative humidity	24.6	37.2	30.9	4.7
Pressure [bar]	Atmospheric pressure	0.993	1.020	1.001	0.01
Flow rate [g/sec]	Mass flow rate of air	2.2	2.5	2.3	0.1
	Mass flow rate of fuel	0.1	0.2	0.1	0.004

* For 3 days at a constant atmospheric pressure of 0.996 bar

3.3 Fuels investigated

Fuels of known RONs, chemical and physical properties but with different chemical composition were selected for the investigation. The test fuels were divided into three sets. Firstly, two commercial highly aromatic gasoline fuels of RONs of 97 and 91.3, respectively, were obtained from Haltermann Carless UK LTD. Secondly, an oxygenated gasoline blend, A 5 % (V/V) ethanol and reference gasoline with RON of 90.9 was blended and delivered by BP Formulated Products Technology, UK. Lastly, Primary Reference fuels (PRFs) were prepared in-house by blending n-Heptane into iso-Octane on a volumetric basis corresponding to the required RON, varying the percentage of n-Heptane (3%, 10% and 15%) to produce PRFs of RON 97, 90 and 85, respectively. Both n-Heptane and iso-Octane with GC purity of 99% and 99.8%, respectively, were purchased from MERCK CHEMICALS.

Table 6 summarises the physical and chemical properties of the test fuels and also of the molecules utilised in preparing the test blends: Ethanol, n-Heptane and iso-Octane. In Table 6, it can be seen that the RON values of the fuels investigated fall in the range of 97 and 85. Two fuels; Gasoline 97 and PRF 97 possessed equivalent RON, while the PRF 85 had the lowest RON value of 85. The other fuels G90.09+5%(V/V) Ethanol, Gasoline 91.3, and PRF90 were distributed between the upper and lower borders of the RON range with small differences in their RON values; 93.7, 91.3 and 90, respectively.

Table 6: Physical and chemical properties of the test fuels.

Fuels	Density[a] g/cm3	Heat of vaporization[b] kJ/mol	H/C[c]	O/C[c]	Stoichio-metric AFR[c]	Calorific value[d] MJ/kg	RON[e]
PRF 85	0.693	---	2.255	0.0	15.14	---	85
PRF 90	0.694	---	2.254	0.0	15.14	---	90
PRF 97	0.695	---	2.251	0.0	15.13	---	97
Gasoline 90.9*	0.744	---	1.864	0.0	14.56	42.95	90.9
Gasoline 91.3	0.731	---	1.822	0.002	14.52	43.44	91.3
Gasoline 90.9 + 5% (V/V) Ethanol	0.746	---	1.901	0.016	14.3	---	93.7
Gasoline 97	0.750	---	1.708	0.008	14.19	42.78	97
iso-Octane*	0.692	35.14	2.250	0.0	15.13	44.31	100
n-heptane*	0.680	36.57	2.286	0.0	15.18	44.57	0
Ethanol*	0.789	42.32	3.000	0.5	9.00	26.8	108.6

a = Data provided by the supplier for gasoline fuels, measured for the PRF blends at T= 20 C, and taken from U.S. National Library of Medicine for iso-Octane, n-Heptane and Ethanol (2022).

b = Data taken from U.S. National Library of Medicine, at 25 ◦C (2022).

c =Data provided by the supplier for gasoline fuels, calculated for the PRF blends, iso-Octane, n-Heptane and Ethanol.

d = Net calorific values as provided by the supplier for gasoline fuels and taken from NIST Chemistry WebBook for the other fuels (2022).

e = Data provided by the supplier for gasoline fuels, calculated for the PRF blends and taken from (Vallinayagam et al., 2017) for Ethanol.

* Those molecules were not tested on their own, however, the data provided for reference as they were utilised as blending components with gasoline fuels.

3.4 Selection of a representative knocking combustion cycle

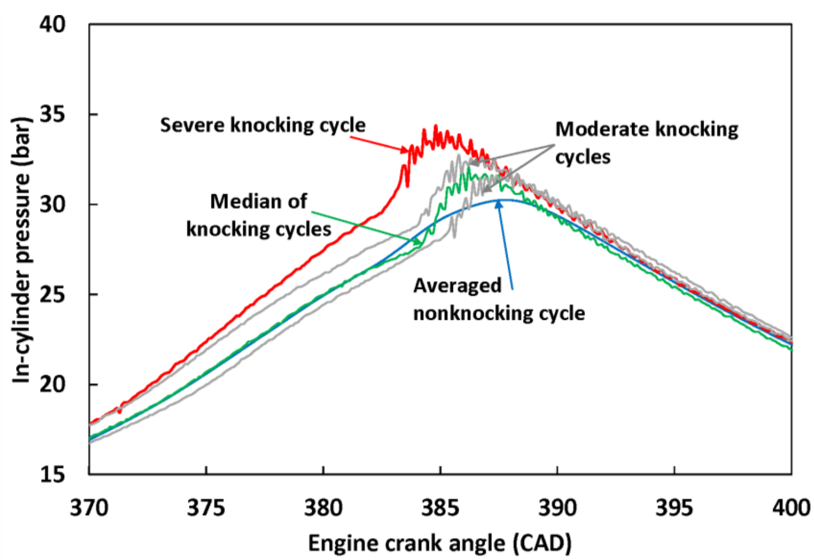

Figure 2: In-cylinder pressure for a typical knocking test of Gasoline 91.3 tested at stoichiometric λ, and engine CR and speed of 7.38 and 600 rpm, respectively.

Figure 2 shows an example of a knocking test conducted during the investigation of the reference gasoline 91.3 test fuel. The engine was operated at the steady-state conditions of 600 rpm, WOT and stoichiometric air-fuel ratio, with the engine compression ratio gradually increased from 6.91 to find the knock limit of the fuel at the required KFRQ.

As can be seen in Figure 2, the engine started to knock as the engine CR increased to 7.38, producing a KFRQ of 8% (four random knocking cycles out of 50 consecutive combustion cycles).

It can be seen, in Figure 2, that all non-knocking cycles were isolated, grouped, averaged and plotted, shown in blue, while the four random knocking cycles were plotted individually and evaluated for knock characteristics. The knocking combustion cycles show differences in knock induced pressure oscillations, peaks and time of occurrence relative to one another (Figure 2). Therefore, to find a representative knocking combustion cycle for the test fuel that could be used to describe the knocking combustion parameters of a given fuel, the median cycle of the knocking cycles was selected. In the case the total number of knocking combustion cycles was even, the selected representative cycle is that which has the amplitude immediately after the median, see Table 7. The amplitude of bandpass filtered in-cylinder pressure at the first knock-point and time of occurrence in crank angle degree were found as representative knocking characteristics of the selected knocking combustion cycle for a test fuel.

Table 7: A summary of knocking combustion cycles analysis of Gasoline 91.3 tested at stoichiometric λ, and engine CR and speed of 7.38 and 600 rpm, respectively.

Knocking combustion cycles number	#7	**#19**	#41	#48	Median	Values of the Selected cycle
Amplitude of in-cylinder pressure at first knock-point (bar)	0.545	**0.556**	0.524	0.56	0.551	0.556

Time of first knock-point (CAD)	385.5	**386.2**	385.5	383.7	385.5	386.2

4 Results and Discussion

4.1 Knock resistance

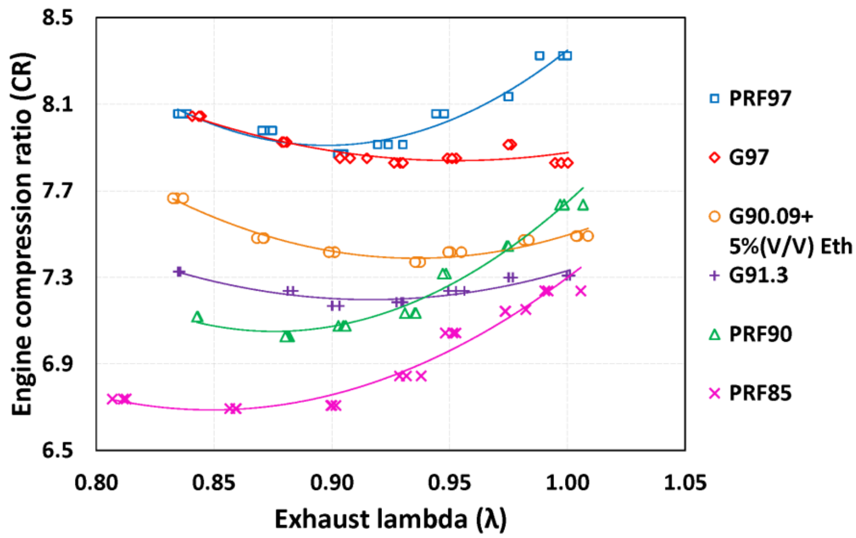

Figure 3: Operating limit of engine CR of the PRFs and gasoline fuels at varying λ between 1.00 and 0.8.

Figure 3 shows the operating limit of the engine compression ratio (CR) for the fuels investigated at different air-fuel ratios (exhaust lambda λ). The operating limit of the engine CRs at λ =1 and the other richer λ values were found at KFRQ of 10% and 30%, respectively (Section 3.2). In Figure 3, in general, it can be seen that the engine CR operating limit increases as the RON of fuels increases. Hence, fuels with high RON such as Gasoline RON97 (G97) and PRF97, which are of higher knock resistance, were able to be tested at a higher engine CR prior to observation of the same frequency of knock as compared to other fuels investigated. This correlation between the ability of fuels to resist knock (the octane number) and the operating limit of engine CR was expected and agrees with the concept of the standard test method for research octane number of spark-ignition engine fuels (ASTM Int., 2019).

It can also be seen, in Figure 3, that the operating limit of engine CR was affected by changing the exhaust lambda λ. In general, for all fuels, engine CR decreases as the mixture becomes richer to a certain limit and subsequently increases as the mixture becomes richer still in order to maintain the same level of knocking frequency. Similar observations have been made in a CFR engine by other researchers (Brock and Stanley, 2012; Wang *et al.*, 2017; Montoya *et al.*, 2018; Hoth *et al.*, 2019). It has been suggested that the influence of varying exhaust lambda on the engine CR can be explained as follows: initially, increasing fuel supply to the engine results in a richer mixture, which increases the burning rate and promotes knock (Chen and Raine, 2015). Furthermore, as a mixture becomes more richer, $\lambda < 0.97$, at a constant throttle position, it means there is more fuel available to be burned and release energy, leading to an increase in combustion and in-cylinder wall temperatures due to increased heat transfer. This effect on the in-cylinder charge temperature persists from cycle to cycle; as the in-cylinder wall temperature increases, more heat is transferred to the in-cylinder charge during intake and compression strokes. Therefore, reaction rates during the end-gas autoignition process are increased through elevated temperatures, decreasing the ignition delay time (Gauthier *et al*., 2004) and hence, autoignition in the end-gas occurs more easily (Bolt and Henein, 1969; Dec and Sjöberg, 2004). As a result, the operating limit of engine CR must be lowered so as to offset the additional in-cylinder temperature gained by mixture enrichment, in order to reduce the severity of the resultant knock. However, Figure 3 also shows that beyond a certain level of mixture richness, varying between fuels in the range $\lambda = 0.85$ to 0.95, a further increase in fuel mass increases engine CR. This can be attributed to insufficient availability of oxygen to fully oxidise the fuel, with combustion therefore becoming oxygen limited, leading to a decrease in the temperature after compression as well as the burning rate, consequently increasing the ignition delay of the end gases (Machrafi *et al.*, 2007; Zheng *et al.*, 2019). Accordingly, an increase in engine CR operating limit is required so that the same knocking frequency is maintained.

From Figure 3, it can be seen that the effect of exhaust lambda λ on the operating limit of engine CR for PRFs is different as compared to gasoline fuels. Overall, it appears that the PRFs are more sensitive to changes in the mixture strength, especially in the range between λ=1 and $\lambda = 0.90$. This observation is even more pronounced when comparing two fuels of equivalent octane rating, for example, PRF97 and Gasoline 97. At $\lambda = 1$, the PRF97 displayed a significantly lower knock propensity as it was able to resist knock until a higher compression ratio than gasoline 97 by 0.5 unit. However, this divergence in engine CR operating limit between the two fuels decreases as the mixture becomes richer, until both fuels show a similar engine CR operating limit at around $\lambda = 0.9$. Similar observations can be made for the other PRFs (90 and 85). At λ=1, the PRF90 showed a higher knock limit than the fuels Gasoline 91.3 and G90.09+5%(V/V) Ethanol, which have higher RON by 1.3 and 3.7 units, respectively. Similarly, the

PRF85, at λ=1, was able to exhibit a knock resistance similar to Gasoline 91.3, which has 6.3 units of RON higher than it. Therefore, the results suggest that at stoichiometric and slightly rich conditions, PRFs possess higher knock resistance than expected relative to gasoline fuels with comparable or higher RON.

The dissimilar effect of varying exhaust lambda λ on the knock tendency of the gasoline fuels and the PRFs is a point of interest and can be discussed by referring to the effect of the fuel composition. The PRFs investigated are highly iso-paraffinic fuels as they consist of high concentrations of iso-octane blended with n-heptane. However, gasoline fuels contain about 30 %(m/m) aromatic compounds along with varying proportions of paraffins, iso-paraffins, olefins, naphthenes molecules, giving gasoline fuels an octane sensitivity of about 10 in comparison to 0 for PRFs (Sluder *et al.*, 2016). A similar experimental observation of the dissimilar knock tendencies of iso-paraffinic and aromatic fuels was reported by Hoth *et al.*, (2019).

According to Iqbal *et al.*, (2011), the presence of olefins and aromatics in fuels such as gasoline changes significantly the chemical kinetics of the fuel oxidation process compared to paraffinic fuels; in contrast to PRFs olefins and aromatics fuels do not exhibit NTC. It was observed experimentally by Iqbal *et al.*, (2011) that PRFs experience an increase in cool flame activity during first stage ignition as the mixture becomes richer due to an increase in energy release, leading to initiation of a second stage ignition. Therefore, the overall ignition delay was decreased much more than olefins and aromatics fuels (Iqbal *et al.*, 2011). A similar observation was reported by Dec and Sjöberg (2004) suggesting that fuels with cool-flame chemistry such as PRFs require immediate compensation in engine operating conditions, such as lowering the engine wall temperature, as the mixture becomes richer; otherwise, the control of combustion will be difficult. These previous observations explain the necessarily sharp decrease in the operating limit of engine CR for PRFs apparent in Figure 3 as lambda becomes increasingly rich.

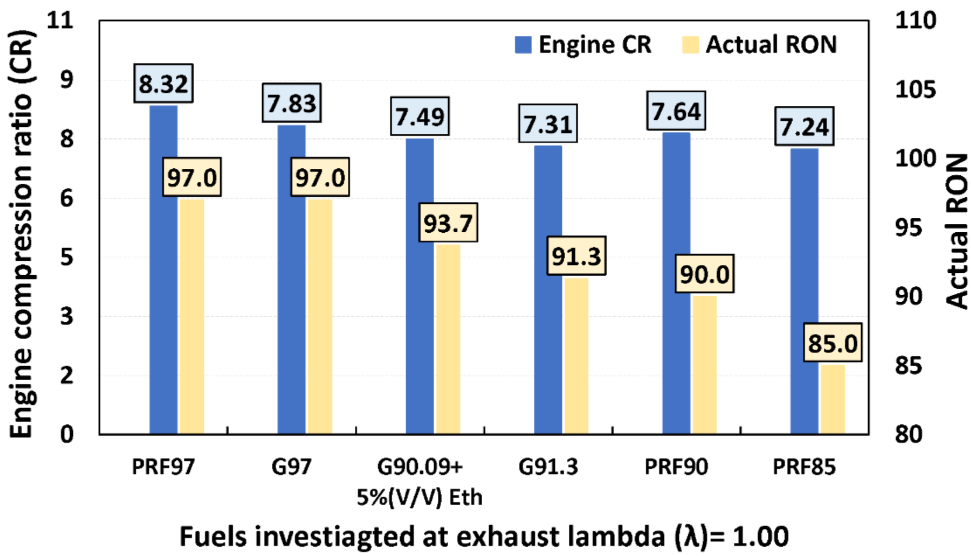

Figure 4: Operating limit of engine CR and RON values of the PRFs and gasoline fuels investigated at λ=1.

Figure 4 shows a comparison of the operating limit of the engine CR obtained for the known-RON PRF and gasoline fuels at stoichiometric λ. It is known, by definition, that there is a slightly non-linear increase of the operating limit of engine CR with increasing RON of a given fuel (ASTM Int., 2019). However, it can be seen in Figure 4 that, as was discussed previously in the context of Figure 3 due to the chemical composition of the fuels investigated, the iso-paraffinic fuels, such as PRF 97 and PRF90, can be operated at higher engine CRs relative to fuels with similar RON but of composition including aromatic compounds, such as Gasoline 97, G90.9+5Eth and Gasoline 91.3. It can be seen that PRF97 operated at a higher engine CR than Gasoline 97 by 0.49 unit. Also, while the engine CR operating limit decreased with decrease in RON from Gasoline 97, to G90.9+5Eth and Gasoline 91.3, PRF90 showed a higher engine CR than the aforementioned fuels despite a lower RON value.

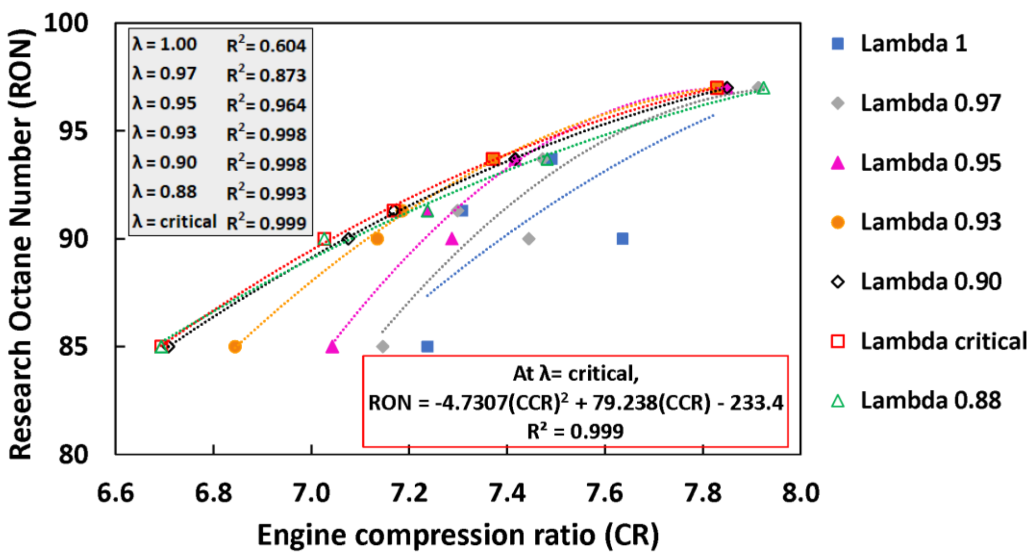

Figure 5: Relationship between the operating limit of engine CR and RON value of the PRFs and gasoline fuels at different exhaust λ.

Figure 5 shows a comparison of the relationship between the operating limit of the engine CR and RON values for the PRF and gasoline fuels at different exhaust lambda λ between 1.00 and 0.88. It can be seen that the trend obtained at stoichiometric λ shows no correlation and does not reflect the theoretical relationship between engine CR and RON of the fuels. Although the trend becomes more representative as the fuels were tested at richer mixtures, exhaust λ ≈ 0.9, each fuel has a particular value of exhaust λ, as was observed in Figure 3, which causes its minimum operating limit of engine CR (CCR). These values of exhaust λ for all fuels investigated were selected and subsequently referred to as the critical λ and engine CR (CRR) values. This combination of critical λ and critical engine compression ratio CCR were found to provide the best correlation, R^2=0.999, between the RON of a given fuel and its knock-limit engine compression ratio CRR despite the difference in the chemical composition.

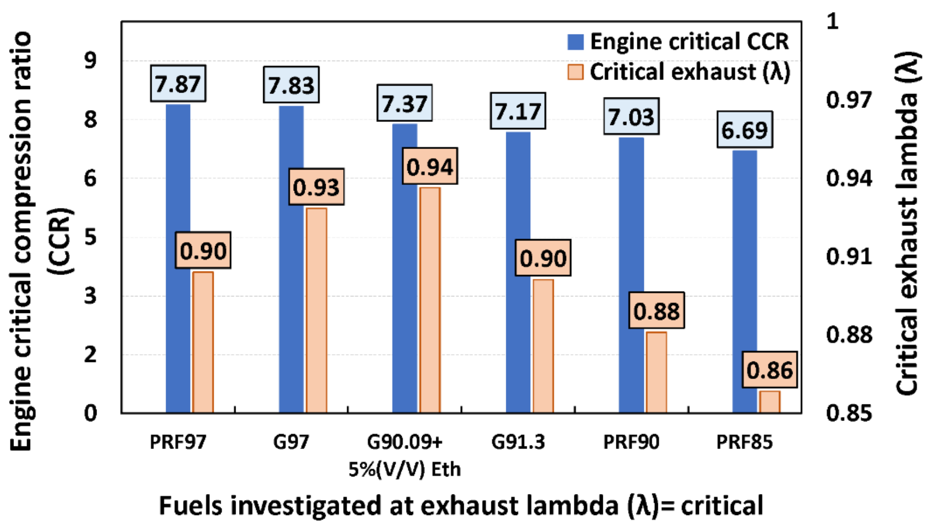

Figure 6: A comparison of the critical operating limit of engine CR and value of critical λ of the PRFs and gasoline fuels investigated.

Figure 6 shows the critical operating limits of engine CR (CCR) of the PRFs and gasoline fuels while operating the critical λ values. In contrast to Figure 4, which made a similar comparison but at λ = 1, it can be seen that the order of the fuels in terms of RON agrees with the determined operating limit of engine CR (CCR), in spite of the varying fuel composition. For example, the difference between the engine CR for PRF97 and Gasoline 97 is reduced significantly from 0.49 to 0.04 units of CR. In addition, PRF90 displays as expected a lower engine CCR compared to G90.09+5%(V/V) Ethanol and Gasoline 91.3.

With regards to the effect of exhaust lambda λ, it can be seen that most of the fuels investigated have a critical λ at very rich mixtures in the range between 0.90 and 0.86, excluding gasoline 97 and the gasoline with ethanol blend (G90.09+5%(V/V) Ethanol) which they have a critical λ at less rich mixtures of 0.93 and 0.94, respectively. These findings agree with the values available in the literature, suggesting that blends including ethanol have a critical λ around 0.93, while iso-paraffinic fuels, PRFs, tend to have a higher knock intensity in the range from 0.90 to 0.88 (Kolodziej, 2017; Foong *et al.*, 2017). It is interesting to see that when considering the PRFs, there is a trend of decreasing critical lambda with decreasing RON. This can be attributed to the increase in the level of n-heptane, which is known to be significantly more reactive at low temperature conditions. The occurrence of knock is less sensitive to oxygen availability as the oxygen that is available is more likely to be consumed by heptane present. Therefore, the increasing temperature with increasing richness becomes the dominant factor.

4.2 Knocking combustion characteristics

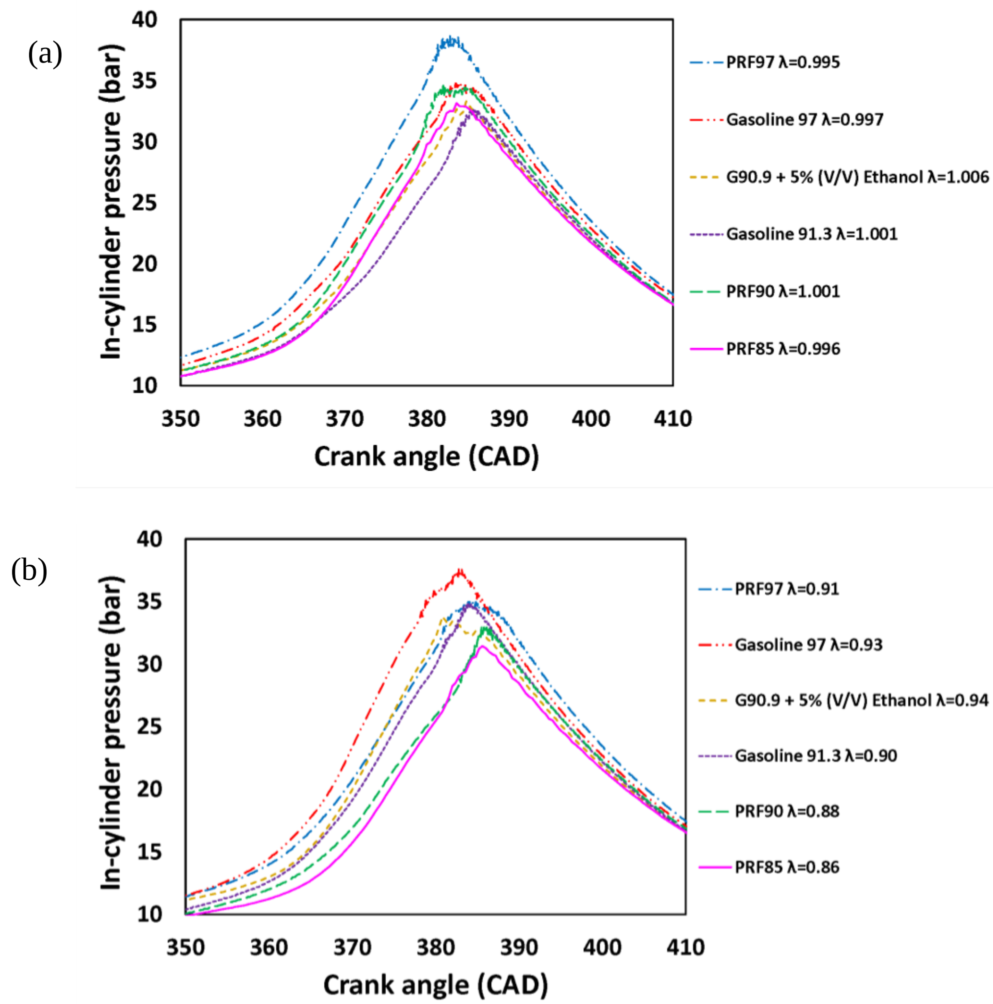

Figure 7: In-cylinder pressure of the representative knocking combustion cycles of the PRFs and gasoline fuels tested at operating limit of engine CR at (a) λ=1 and (b) λ=critical.

Figures 7 (a) and (b), show the in-cylinder pressure for the representative knocking combustion cycles of the PRF and gasoline fuels tested at the operating limit of engine CRs at λ=1 and λ=critical, respectively. It can be seen, in Figure 7 (a), that at stoichiometric λ=1 the iso-paraffinic fuels (PRFs) displayed higher levels of in-cylinder pressure relative to the aromatic fuels (gasoline fuels) although all fuels operated at engine CRs that produced the same knocking frequency. This means that, for example, PRF97 reached the knocking frequency threshold at a peak in-cylinder pressure higher than Gasoline 97 by about 10%. The results also show that PRF90 and PRF85 exhibited a peak in-cylinder pressure equivalent to aromatic fuels of approximately seven units higher octane number. These observations were expected as the PRFs, at λ=1, operated at a much higher engine CR in comparison to gasoline fuels, as was discussed in the context of Figure 4.

Comparing the fuels investigated at their critical conditions of exhaust lambda λ and engine CR shows a contrary observation to that at λ=1. It can be seen in Figure 7 (b) that the iso-paraffinic fuels (PRFs), for example PRF97 and PRF90, tend to reach the pre-determined knocking threshold at an in-cylinder pressure much lower than the aromatic fuels Gasoline 97 and Gasoline 91.3, respectively. It is worth noting that, at the critical test conditions, the addition of ethanol to gasoline fuel causes the knock to occur at lower in-cylinder pressure compared to Gasoline 91.3, even though it was operated at a higher engine CR. This could be attributed to the faster burning velocity gained by the addition of ethanol, advancing the peak of in-cylinder pressure closer to the engine TDC combustion occurring at a smaller volume (Turner *et al.*, 2011;Jiang *et al.*, 2017).

(a)

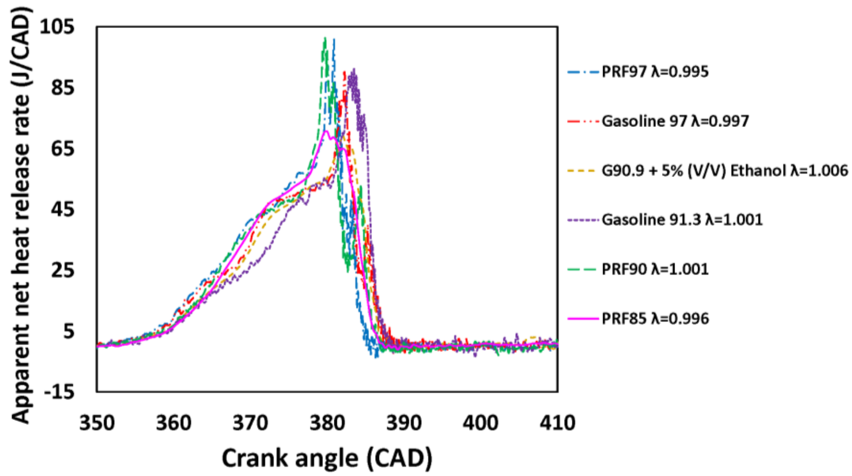

(b)

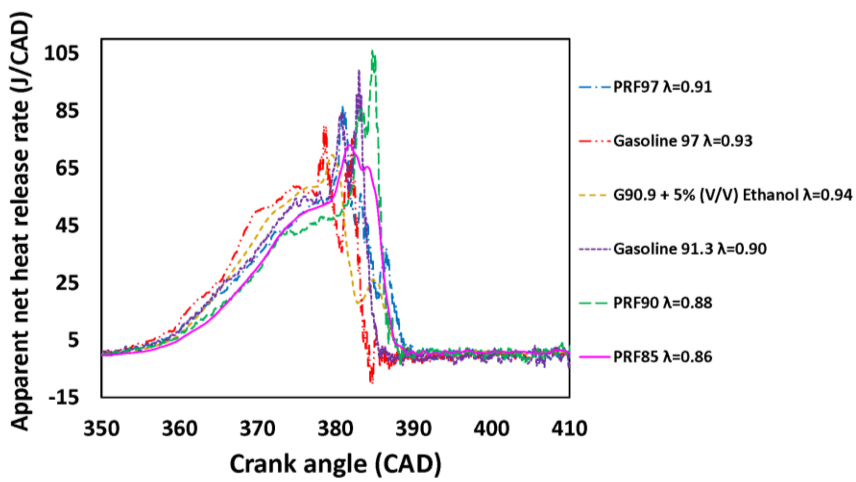

Figure 8: Apparent net heat release rate of the representative knocking combustion cycles of the PRFs and gasoline fuels tested at operating limit of engine CR at (a) λ=1 and (b) λ=critical.

The apparent net heat release rate of the representative knocking combustion cycles of the fuels investigated at the operating limit of engine CRs at λ=1 and λ=critical are shown in Figures 8 (a) and (b), respectively. At λ=1, in general, all fuels experienced multiple peaks of heat release due to knocking combustion between 377 and 386 CAD, with the iso-paraffinic fuels (PRFs) advanced relative to the aromatic fuels. This is also apparent in the in-cylinder pressure traces, Figures 7 (a) and (b), and can be attributed to testing of the PRFs at a higher engine CR (Figure 3). The results also show that the PRFs produced higher cumulative energy release rate by approximately 10% than the gasoline fuels, due to the higher calorific value of the former. However, at the critical λ operation, it can be seen, in Figure 8 (b), that the aromatic fuels tend to knock earlier than the iso-paraffinic fuels, as the initial peaks of heat release (present due to knock in the end-gas zone) occur approximately 1.5 CAD, earlier.

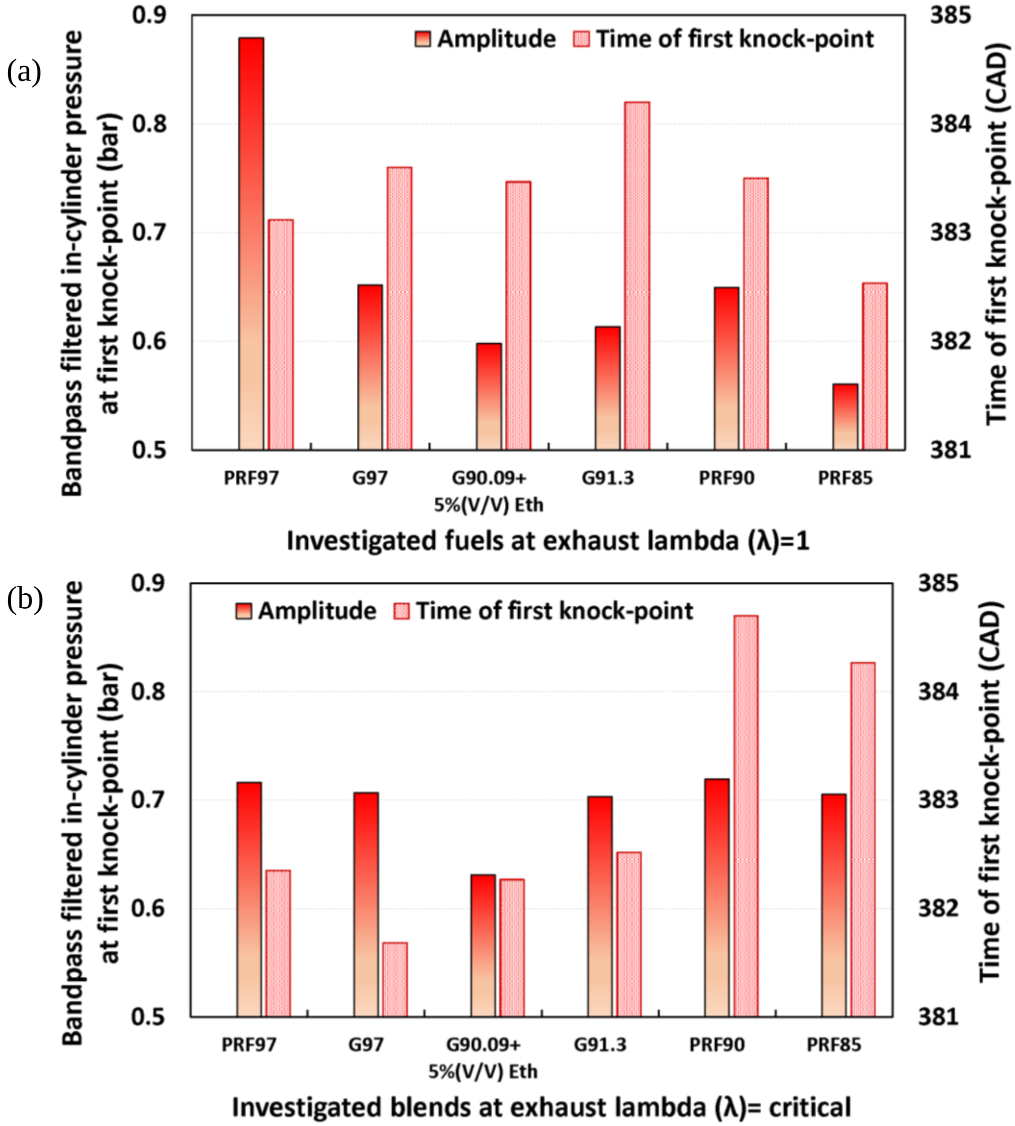

Figure 9: Amplitude of bandpass filtered in-cylinder pressure and angle at first knock-point of the representative knocking combustion cycles of the PRFs and gasoline fuels tested at operating limit of engine CR at (a) λ=1 and (b) λ=critical.

Detection of knock during the experiments was undertaken by application of a bandpass filter to the in-cylinder pressure data (as described in Section 3.1). Figures 9 (a) and (b) show the increase in amplitude of the bandpass filtered in-cylinder pressure and the time of occurrence for the first knock-point of the representative knocking combustion cycles of the PRFs and gasoline fuels tested at the operating limit of engine CRs at λ=1 and λ=critical, respectively. In general, increases in the amplitude of the in-cylinder pressure of the representative knocking cycles are shown to be lower at λ=1 than at λ=critical, except PRF97 which required the highest engine CR in order to reach the pre-determined knock threshold (Figure 3). This characteristic is also apparent in Figure (7 a), where fluctuations are apparent at the peak in-cylinder pressure of PRF97. However, at λ=1, it can be seen that the increase in amplitude for the iso-paraffinic fuels decreases significantly by 26% and 36% as the n-heptane content increases from 3% to 15%, respectively. On the other hand, the Figure 9 shows a slightly higher increase in amplitude in the case of Gasoline 97 relative to Gasoline 91.3, while the addition of ethanol (G90.09 + 5% (V/V) Eth) reduces it compared to Gasoline 97 and Gasoline 91.3.

Additionally, Figures 9 (a) and (b) show that the time of the first knock-point is delayed for most of the fuels at λ=1 compared to λ=critical, except PRF90 and PRF85. These observations can likely be attributed to the increase in the burning velocity of the fuels at the richer λ=critical conditions relative to λ=1, which increases the rate of combustion and reduces its duration (Figure 8). As a result, at the critical lambda operating condition, which is rich for all fuels (Figure 6), the amplitude of in-cylinder pressure shows little variation despite the differences fuel composition, (with the exception of the ethanol/gasoline blend). The addition of ethanol to fuels was found to reduce peak-to-peak in-cylinder pressure fluctuations which may be the reason why the amplitude of in-cylinder pressure is lower than the other fuels. These observations are in agreement with the study of (Kolodziej, 2017). With regards to the delayed time of the amplitude of in-cylinder pressure for PRF90 and PRF85, these fuels were seen in (Figure 7 b) to reach a peak in-cylinder pressure later compared to the other fuels investigated as they were operated at lower engine CR corresponding to their RON values.

Figures 10 (a) and (b) show the burn duration of the combustion characteristics CA10, CA50, CA90, in addition to the interval to the first knock-point relative to the spark timing for the knock representative cycle of the fuels investigated at the operating limit of engine CRs at λ=1 and λ=critical, respectively. It can be seen that at λ=1, the burn duration CA10 increases gradually by less than a CAD as the RON of the aromatic fuel decreases. At the same time, a more significant increase, (by about 1.5 CAD), is apparent for the iso-paraffinic fuels as the RON decreases from 97 to 90 and then to 85, with PRF85 exhibiting the longest CA10 burn duration of 21 CAD.

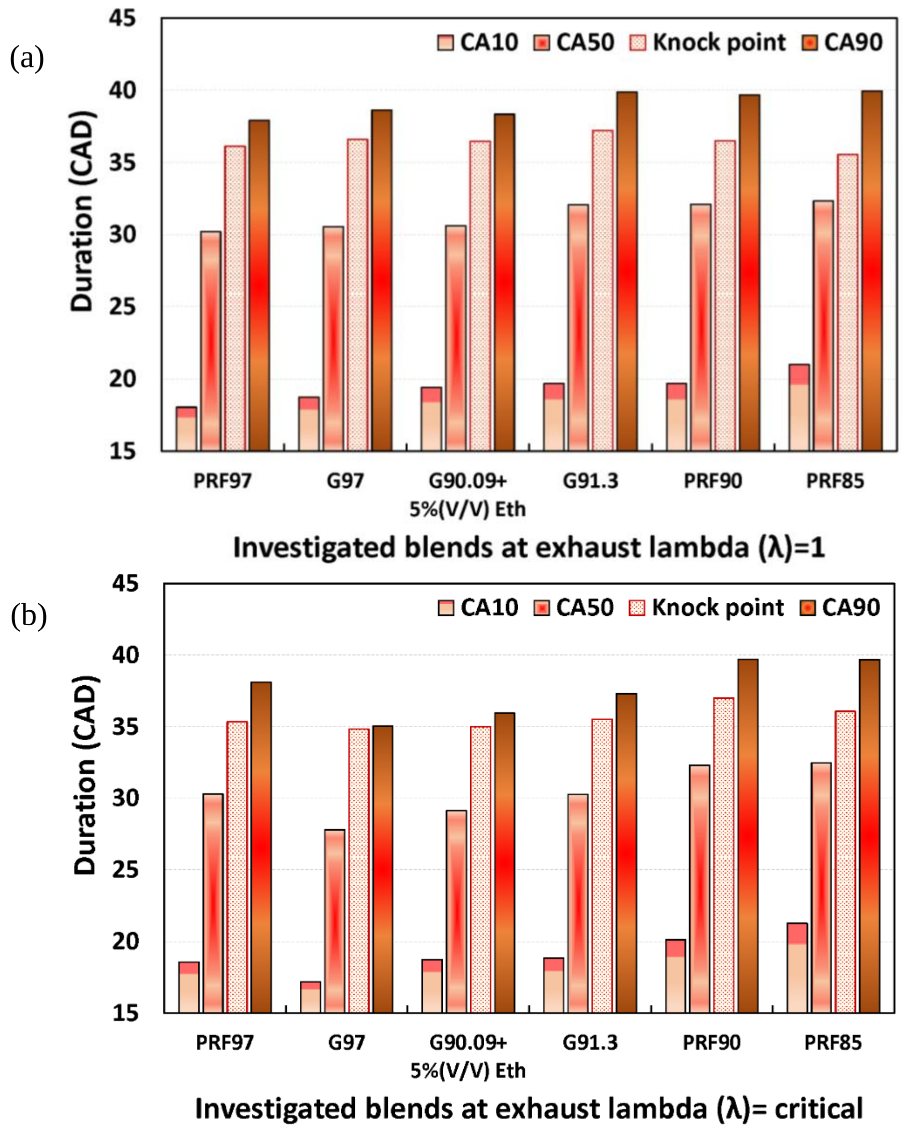

Figure 10: Durations of CA10, CA50 and CA90 of the representative knocking combustion cycles of the PRFs and gasoline fuels tested at operating limit of engine CR at (a) λ=1 and (b) λ=critical.

As for the CA50 and CA90 durations, fuels with high RONs such as PRF97, Gasoline 97 and G90.09+5%(V/V) Ethanol displayed comparably shorter durations of about 2 CAD less in comparison to fuels with lower RONs such as Gasoline 91.3, PRF90 and PRF85. At constant RON, it can be seen that PRF 97 exhibited slightly lower burn durations of CA50 and CA90 as it was operated at a higher compression ratio than Gasoline 97. It can be observed that, at a constant λ=1, as the RON of the fuels decreases, iso-paraffinic fuels, especially PRF97 and PRF90, experience a more considerable delay in flame initiation, combustion rate and overall combustion durations than aromatic fuels. However, at a comparable RON value, iso-paraffinic fuels show a slightly shorter duration as they require operation at a higher engine CR than aromatic fuels to achieve the same knock frequency and intensity (Figure 3). The addition of ethanol to gasoline shows a slight decrease in the CA10 duration, while a significant reduction (by about 1.5 CAD) can be seen in the combustion phasing CA50 and CA90 compared to non-oxygenated gasoline (Gasoline 91.3). With regards the interval to the first knock-point, it can be observed that the iso-paraffinic fuels displayed shorter durations relative to the aromatic fuels, in agreement with Figure 8 in which the PRFs were observed to exhibit peaks of ANHRR earlier than the aromatic fuels.

Figure (10 b) shows the same combustion parameters where the fuels were tested at their critical conditions of engine CR and λ ratio. Overall, as was seen at the constant λ=1, an increase in the burn duration CA10 with decreasing fuel RON is apparent. However, this increase is also visible in the other burn durations, CA50 and CA90. It is interesting to note that the duration of CA10 of the iso-paraffinic fuels become slightly longer than that found at λ=1, while no significant changes in the durations of CA50 and CA90 can be seen. However, the aromatic fuels experience, at the critical conditions relative to λ =1, considerable reduction by about 3 CAD in all durations.

Therefore, it can be summarised that iso-paraffinic fuels have more prolonged combustion initiation and development durations than the aromatic fuels at critical knock operating conditions of engine CR and air-fuel ratios. This explains the late occurrence of ANHRR peaks for the iso-paraffinic fuels, shown in Figure (8 b), compared to the aromatic fuels, which tend to have faster heat release and earlier knocking peaks. The results of knock-point durations show that iso-paraffinic fuels tend to knock at an angle closer to CA50. In contrast, the aromatic fuels resist knocking for a more extended period, with a knock-point much closer to the end of the combustion phase.

4.3 Fuel flow characteristics

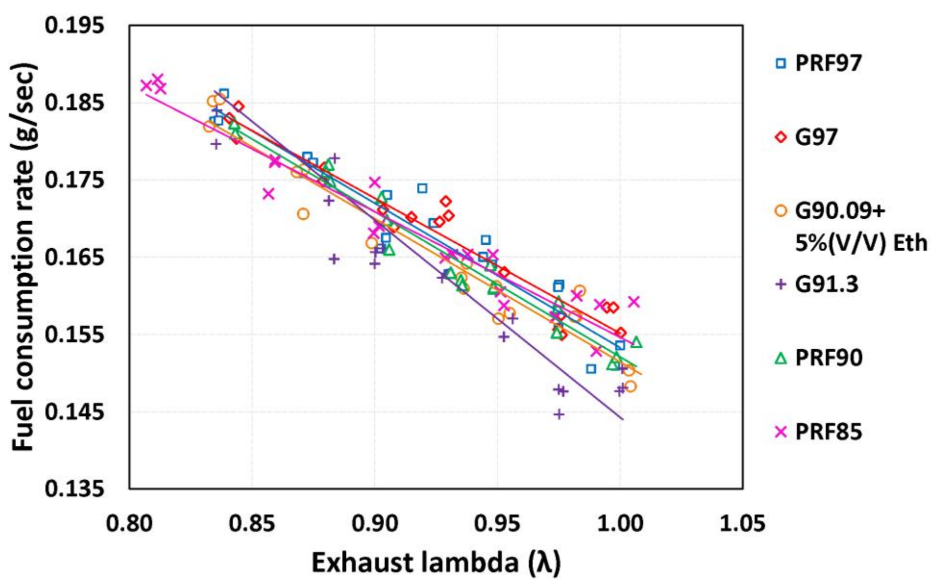

Figure 11: Fuel consumption rate of the investigated PRFs and gasoline fuels tested at operating limit of engine CR and varying exhaust λ.

Figure 11 shows the fuel consumption rates, over the operating range of λ, for the PRFs and gasoline fuels. Overall, all fuels exhibit comparable consumption rates with a linear increase of about 25% when increasing the mixture stoichiometry from (λ=1 to λ= 0.82). However, fuels with higher heating values and lower stoichiometric AFR, such as Gasoline 91.3 and G90.09+5%(V/V) Ethanol, tend to display slightly lower fuel consumption rates relative to the other fuels. Of the PRFs, PRF85, which has the highest content of *n*-heptane, exhibits a relatively higher fuel flow rate compared to PRF97 and PRF90. Table 8 shows the indicated specific fuel consumption rates of the fuels investigated at exhaust λ=1.

Table 8: Indicated specific fuel consumption rates of the fuels investigated at exhaust λ=1.

Fuels	PRF97	G97	G90.09 + 5%(V/V) Eth	G91.3	PRF90	PRF85
ISFC (g/kWh)	254.8	271.0	277.3	273.8	267.8	289.0

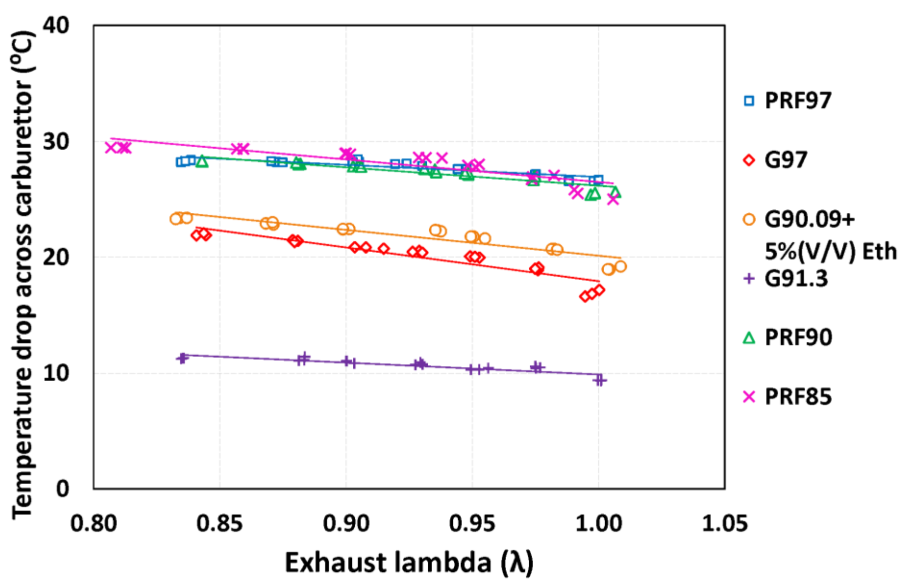

Figure 12: Temperature drop across the carburettor during supply of the investigated PRFs and gasoline fuels tested at operating limit of engine CR and varying exhaust λ.

Figure 12 shows the temperature drop across the carburettor during the supply of the fuels investigated over the entire operating range of exhaust λ. Overall, it can be seen that the reduction in temperature increases with the increase of fuel supply to the engine, as is expected given that there is more fuel to be mixed with the hot air causing a further reduction in the charge temperature. The heat of vaporisation (HoV) of each fuel plays a significant role here, therefore, it is expected there is a different reduction in temperature among the fuels investigated. For PRFs, it can be seen in Figure 11, an increase in fuel flow rate with increasing n-heptane content. It is known that relative to iso-octane, n-heptane has a slightly higher (HoV) by about 1.4 kJ/mol. As a result, a slight increase in the temperature drop can be seen as the *n*-heptane content in the PRFs increases. With regard the gasoline fuels, it is interesting to see that the addition of 5% (V/V) of ethanol, which has a higher HoV than iso-octane, increased the temperature drop by about 50% compared to Gasoline 91.3. It can also be seen that Gasoline 97 displayed a significant reduction in the temperature drop relative to Gasoline 91.3, but of slightly lower magnitude than that exhibited by G90.09+5%(V/V) Ethanol. The cooling effect of fuels is an essential factor for suppressing engine knock. As for ethanol, it is quantitatively described as an equivalent octane number (Wang, Zeraati-Rezaei, *et al.*, 2017).

5 Conclusions

In this study, the effect of varying air-fuel ratio and fuel composition on knock resistance during spark-ignition combustion were experimentally investigated. In addition, knocking combustion characteristics and cooling effect of the test fuels were evaluated and compared. It was found that the determination of the operating limit of engine CR, at the targeted knocking frequency, depended significantly on the air-fuel ratio and the chemical composition of a test fuel. By investigating these effects, the following conclusions can be drawn:

- A richer mixture exhibited knocking combustion at a lower engine CR than a leaner mixture, due to the decrease in ignition delay caused by the increase in end- gas reaction rates at the elevated in-cylinder temperature present when enriching the mixture. However, introducing too much fuel increased the engine CR required to maintain the same level of knocking frequency, attributable to an increase in the ignition delay with decreasing in-cylinder temperature and burning rate as a result of insufficient oxygen availability to fully oxidise the fuel.
- Highly aromatic fuels were less sensitive to changes in exhaust lambda λ than highly iso-paraffinic fuels and, exhibited less variation in the operating limit of engine CR at varying exhaust lambda λ. However, at the same operating condition of exhaust lambda λ, especially at stoichiometric and slightly rich λ, iso-paraffinic fuels displayed greater knock resistance than highly aromatic fuels of the same RON values, requiring operation at a higher engine CR in order to exhibit the same level of knocking frequency.
- The effect of fuel composition on the determination of the operating limit of engine CR, at the targeted knocking frequency, indicated the importance of comparing test fuels with different chemical composition at their critical exhaust

lambda λ rather than at fixed exhaust lambda λ. Thus, a great degree of correlation remained between the operating limit of the engine CR and known RON values despite differences in fuel composition.

Regarding the effect of chemical composition of the test fuels on knocking combustion characteristics, it was found that:

- For all fuels, the in-cylinder pressure fluctuations at the critical λ were stronger than at other λ values, attributed to the effect of multiple auto-ignition occurrences that increased the in-cylinder pressure fluctuations. At these conditions, the iso- paraffinic fuels produce higher peak-to-peak in-cylinder pressure fluctuations and peak of heat release rates with longer combustion initiation and development durations, and a propensity to knock at an angle much closer to the mid-point of combustion (CA50) and earlier compared to the aromatic fuels.
- The addition of ethanol to gasoline increased the rate of combustion and decreased peak-to-peak in-cylinder variation compared to PRFs and other gasoline fuels, attributable to the presence of an alcohol functional group.

The effect of chemical composition of the test fuels on the fuel consumption rate and cooling effect, as a temperature drop across the carburettor, while varying the exhaust lambda λ, can be summarised as follows:

- In general, all fuels have a comparable rate of fuel consumption. However, a more significant reduction in temperatures across the carburettor was observed with the PRFs and (G90.09+5%(V/V) Ethanol) fuel, due to their high heat of vaporisation (HoV). It is interesting to note that the addition of 5% (V/V) ethanol to gasoline 90.9 reduced the charge temperature by 50% compared to Gasoline 91.3.

6 References

AlAbbad, M. *et al*. (2017) 'Ignition delay time measurements of primary reference fuel blends', *Combustion and Flame*. Elsevier Inc., 178, pp. 205–216. doi: 10.1016/j.combustflame.2016.12.027.

ASTM Int. (2019) 'Standard Test Method for Research Octane Number of Spark-Ignition Engine Fuel 1', i(C), pp. 1–45. doi: 10.1520/D2699-19.

Bolt, J. A. and Henein, N. A. (1969) 'The Effect of Some Engine Variables on Ignition Delay and Other Combustion Phenomena in a Diesel Engine', *Proceedings of the Institution of Mechanical Engineers, Conference Proceedings*, 184(10), pp. 130–136. doi: 10.1243/pime_conf_1969_184_327_02.

Brock, C. and Stanley, D. (2012) 'The Cooperative Fuels Research Engine: Applications for Education and Research', *Journal of Aviation Technology and Engineering*, 2(1), pp. 130–135. doi: 10.5703/1288284314865.

Chen, Y. and Raine, R. (2015) 'A study on the influence of burning rate on engine knock from empirical data and simulation', *Combustion and Flame*. The Combustion Institute, 162(5), pp. 2108–2118. doi: 10.1016/j.combustflame.2015.01.009.

Coetzer, R. L. J. *et al.* (2006) ‘The estimation of knock-points of fuels by a weighted mean square error criterion’, *Fuel*, 85(12–13), pp. 1880–1893. doi: 10.1016/j.fuel.2006.01.023.

Dec, J. E. and Sjöberg, M. (2004) ‘Isolating the effects of fuel chemistry on combustion phasing in an HCCI engine and the potential of fuel stratification for ignition control’, *SAE Technical Papers*, 2004(724). doi: 10.4271/2004-01-0557.

Foong, T. M. *et al.* (2017) ‘Modeling End-Gas Autoignition of Ethanol/Gasoline Surrogate Blends in the Cooperative Fuel Research Engine’, *Energy and Fuels*, 31(3), pp. 2378–2389. doi: 10.1021/acs.energyfuels.6b02380.

Gauthier, B. M., Davidson, D. F. and Hanson, R. K. (2004) ‘Shock tube determination of ignition delay times in full-blend and surrogate fuel mixtures’, *Combustion and Flame*, 139(4), pp. 300–311. doi: 10.1016/j.combustflame.2004.08.015.

Gómez Montoya, J. P., Amador Diaz, G. J. and Amell Arrieta, A. A. (2018) ‘Effect of equivalence ratio on knocking tendency in spark ignition engines fueled with fuel blends of biogas, natural gas, propane and hydrogen’, *International Journal of Hydrogen Energy*, 43(51), pp. 23041–23049. doi: 10.1016/j.ijhydene.2018.10.117.

Hamilton, L. J. and Cowart, J. S. (2008) ‘The first wide-open throttle engine cycle: Transition into knock experiments with fast in-cylinder sampling’, *International Journal of Engine Research*, 9(2), pp. 97–109. doi: 10.1243/14680874JER02407.

Hoth, A. *et al.* (2019) ‘Effects of lambda on knocking characteristics and RON rating’, *SAE Technical Papers*, 2019-April(April). doi: 10.4271/2019-01-0627.

Huber, K. *et al.* (2013) 'New Test Procedure to Determine Fuel's Knock Resistance', *MTZ worldwide*, 74(7–8), pp. 62–69. doi: 10.1007/s38313-013-0078-4.

Iqbal, A. *et al.* (2011) 'Ignition Delay Correlation for Predicting Autoignition of a Toluene Reference Fuel Blend in Spark Ignition Engines', *SAE International Journal of Engines*, 4(1), pp. 219–234. doi: 10.4271/2011-01-0338.

Jiang, Y. *et al.* (2017) 'Laminar burning characteristics of 2-MTHF compared with ethanol and isooctane', *Fuel*, 190. doi: 10.1016/j.fuel.2016.11.036.

Kalghatgi, G. (2018) 'Knock onset, knock intensity, superknock and preignition in spark ignition engines', *International Journal of Engine Research*, 19(1), pp. 7–20. doi: 10.1177/1468087417736430.

Kalghatgi, G. and Stone, R. (2018) 'Fuel requirements of spark ignition engines', *Proceedings of the Institution of Mechanical Engineers, Part D: Journal of Automobile Engineering*, 232(1), pp. 22–35. doi: 10.1177/0954407016684741.

Kolodziej, C. P. (2017) 'CE-2017-427 Combustion characteristics of various fuels during research octane number testing on an instrumented CFR F1 / F2 engine', 171(4), pp. 164–169. doi: 10.19206/CE-2017-427.

KOLODZIEJ, C. and WALLNER, T. (2017) 'Combustion characteristics of various fuels during research octane number testing on an instrumented CFR F1/F2 engine', *Combustion Engines*, 171(4), pp. 164–169. doi: 10.19206/CE-2017-427.

Machrafi, H. *et al.* (2007) 'HCCI engine modeling and experimental investigations - Part 1: The reduction, composition and validation of a n-heptane/iso-octane mechanism', *Combustion Science and Technology*, 179(12), pp. 2561–2580. doi: 10.1080/00102200701486931.

Naruke, M. *et al.* (2020) 'Investigation of fuel effects on the knock under lean burn conditions in a spark ignition engine', *Fuel*. Elsevier, 282(April), p. 118785. doi: 10.1016/j.fuel.2020.118785.

Ratcliff, M. A. *et al.* (2018) 'Effects of Heat of Vaporization and Octane Sensitivity on Knock-Limited Spark Ignition Engine Performance', *SAE Technical Papers*, 2018-April(April), pp. 10–12. doi: 10.4271/2018-01-0218.

Sluder, C. S. *et al.* (2016) 'Exploring the Relationship Between Octane Sensitivity and Heat-of-Vaporization', *SAE International Journal of Fuels and Lubricants*, 9(1), pp. 80–90. doi: 10.4271/2016-01-0836.

Stradling, R. *et al.* (2016) 'Effect of Octane on Performance, Energy Consumption and Emissions of Two Euro 4 Passenger Cars', *Transportation Research Procedia*. Elsevier B.V., 14, pp. 3159–3168. doi: 10.1016/j.trpro.2016.05.256.

Syrimis, M. and Assanis, D. N. (2003) 'Knocking Cylinder Pressure Data Characteristics in a Spark-Ignition Engine', *Journal of Engineering for Gas Turbines and Power*, 125(2), p. 494. doi: 10.1115/1.1560709.

Turner, D. *et al.* (2011) ‘Combustion performance of bio-ethanol at various blend ratios in a gasoline direct injection engine’, *Fuel*. Elsevier Ltd, 90(5), pp. 1999–2006. doi: 10.1016/j.fuel.2010.12.025.

Wang, C., Zeraati-Rezaei, S., *et al.* (2017) ‘Ethanol blends in spark ignition engines: RON, octane-added value, cooling effect, compression ratio, and potential engine efficiency gain’, *Applied Energy*. Elsevier Ltd, 191, pp. 603–619. doi: 10.1016/j.apenergy.2017.01.081.

Wang, C., Prakash, A., *et al.* (2017) ‘Significance of RON and MON to a modern DISI engine’, *Fuel*, 209(November 2016), pp. 172–183. doi: 10.1016/j.fuel.2017.07.071.

Wang, Z., Liu, H. and Reitz, R. D. (2017) ‘Knocking combustion in spark-ignition engines’, *Progress in Energy and Combustion Science*. Elsevier Ltd, 61, pp. 78–112. doi: 10.1016/j.pecs.2017.03.004.

Zhen, X. *et al.* (2012) ‘The engine knock analysis - An overview’, *Applied Energy*. Elsevier Ltd, 92, pp. 628–636. doi: 10.1016/j.apenergy.2011.11.079.

Zheng, J. *et al.* (2019) ‘Effect of equivalence ratio on combustion and emissions of a dual-fuel natural gas engine ignited with diesel’, *Applied Thermal Engineering*. Elsevier, 146(June 2018), pp. 738–751. doi: 10.1016/j.applthermaleng.2018.10.045.